Title
Studies of Faceting by High Voltage/High Resolution Microscopy

Authors
Westmacott, K.H.
Dahmen, U.

Publication Date
1990

Lawrence Berkeley Laboratory
UNIVERSITY OF CALIFORNIA

Materials & Chemical Sciences Division

National Center for Electron Microscopy

Presented at the Workshop on Interfaces,
Bangalore, India, November 30–December 3, 1989,
and to be published in the Proceedings

Studies of Faceting by High Voltage/ High Resolution Microscopy

K.H. Westmacott and U. Dahmen

January 1990

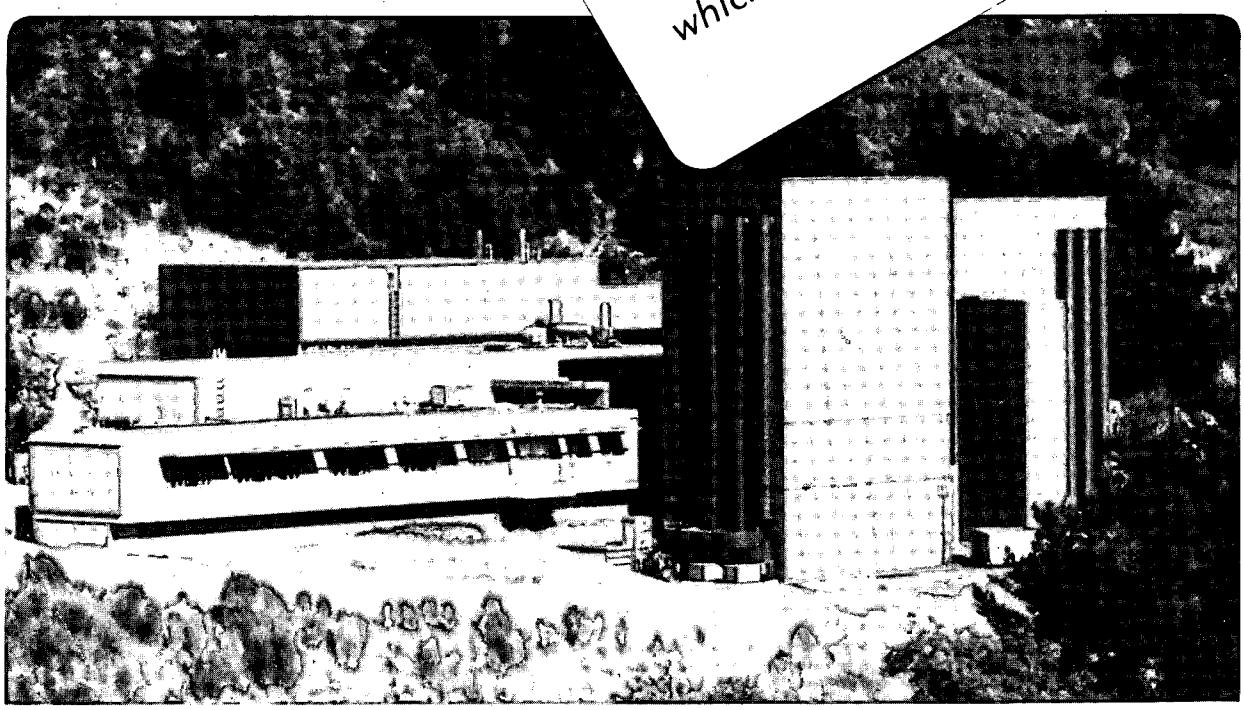

Prepared for the U.S. Department of Energy under Contract Number DE-AC03-76SF00098.

DISCLAIMER

LBL-28627

Studies of Faceting by High Voltage/High Resolution Microscopy

K.H. Westmacott and U. Dahmen

Lawrence Berkeley Laboratory
University of California
Berkeley, CA 94720

January 1990

This work was supported by the Director, Office of Energy Research,
Office of Basic Energy Sciences of the U. S. Department of Energy
under Contract No. DE-AC03-76SF00098.

STUDIES OF FACETING BY HIGH VOLTAGE/HIGH RESOLUTION MICROSCOPY

K.H. Westmacott, and U. Dahmen

National Center for Electron Microscopy
Lawrence Berkeley Laboratory
University of California
Berkeley, CA. 94720

INTRODUCTION

Because numerous properties of materials, such as strength, fracture, creep, are influenced by internal interfaces, fundamental studies of the atomic structure of interfaces can ultimately lead to improvements in the performance of materials. With the advent of transmission electron microscopes with sub-2Å resolution it became possible to make detailed comparisons between experimental images of the atomic structure of interfaces in close-packed metals and simulated structures predicted by theory. However, the stringent experimental conditions that must be satisfied for atomic resolution at interfaces (see Figure 1) is still a severe barrier to widespread application of the technique (1). In general, the optimum conditions for imaging interfaces are found only in specimens prepared by a long and tedious procedure involving orienting, cutting, cleaning and joining single crystals (2). It has been recognized, however, that interfaces with the required special geometry can in some cases be prepared by simpler means (3). One such path is via the Ionized Cluster Beam (ICB) deposition technique pioneered at Kyoto University by Takagi and Yamada (see, e.g. Ref. 4). Using this procedure thin <110> oriented aluminum films with a continuous bicrystal structure ideally suited for high resolution observation have been prepared (5,6,7). Unlike conventionally prepared bicrystals, these heteroepitaxial films contain a large number of 90° tilt boundaries with many different boundary plane orientations.

The purpose of this paper is to describe the various ways in which interface structure is being studied in these materials.

EXPERIMENTAL METHODS

Specimens for the electron microscopy were made from samples of ICB-deposited aluminum on {100} silicon prepared at the Kyoto Ion-Beam Engineering Laboratory, by well established procedures. Discs 3mm in diameter were trepanned from the substrate taking care to protect the thin Al deposited film from damage. The discs were then back-thinned to electron transparency from the silicon side using either a silicon chemical polish followed by brief ion beam cleaning, or by mechanical dimpling followed by more extensive ion-beam thinning. The thickness of the Al deposited film in the present work was 125nm. With the preparation technique used, the TEM specimen consisted of the free-standing ICB Al (wedge-shaped in cross

section) near the hole at the center of the disc (see Figure 2). Further away from the hole the Al remained supported by the silicon substrate.

High resolution images were obtained of grain boundaries in thin regions of the Al marked 1 in Figure 2. Images were also obtained from interfaces found between individual clusters deposited on an amorphous carbon substrate. The JEOL 1000 Atomic Resolution Microscope operated at 800 kV was used for this purpose.

In-situ studies were performed on the Kratos EM 1500 operated at 1500 kV in thicker regions of the foil, marked 2 and 3. This microscope is equipped with a lens-coupled 80mm, low light level, high-resolution Westinghouse TV camera used with a YAG scintillator, and a double tilt, 750°C side entry heating rod.

In addition to the plan view observations a few experiments were conducted on cross section specimens to study the heterophase Al overlayer/Si substrate interface structure. Some differences between these structures and those found when Al/Ge interfaces are formed by a solid state precipitation reaction will be pointed out.

Image processing (8) was used to enhance the high resolution images of discrete clusters to discriminate them from the amorphous substrate.

RESULTS

Interfaces Arising During Cluster Formation or Coalescence

High resolution images have been recorded of widely separated individual clusters of atoms which form on a cold substrate during short (1-10 second) ICB depositions. To minimize complications arising from oxidation of the clusters, silver was used in these experiments. It has been observed (9) that bulk migration of clusters across an amorphous carbon substrate can occur during prolonged aging at room temperature.

Examples of individual single crystal particles and other particles containing single and multiple twins are given in Figure 3. From observations on many particles it is found that internal interfaces in the clusters are invariably coherent $\Sigma 3$ twins. However, because a range of particle sizes is present and the incidence of twinning is not related to the particle size; for example, the smallest particle, Fig. 3b, is pentagonally twinned, whereas the largest, Fig. 3c, contains only a single twin. It appears that the internal twin structure may form in two ways: either during the initial cluster condensation, or by subsequent migration and coalescence of single crystal clusters. Further work is required to clarify this point. In any event, the low energy $\Sigma 3$ coherent twin boundary is clearly the most favored configuration. It is possible that with a sufficiently large number of observations other orientation relationships will be found allowing a comparison with the results of sphere-on-plate type experiments, e.g.(10,11).

Structure of Annealed Continuous Bicrystal Films

A schematic diagram showing the geometric relationship between the ICB aluminum films and a {100} silicon substrate is given in Figure 4. Two <110> orientation variants of the Al develop rotated relative to each other by ~90°. In the resulting continuous bicrystal structure all the grain boundaries close on themselves and no triple points exist. This makes the structure ideal for studying boundary orientation as a function of temperature for a fixed (90°) crystal misorientation.

To study the effect of temperature on the development of facets on the boundaries in the free-standing Al (i.e. with the Si substrate removed) a suitably sized grain was selected and changes in its shape were recorded as the temperature was cycled between 200 and 430°C. At the outset the microstructure was stabilized by heating the specimen to 550°C for 5 minutes. The experiments were carried out on a biaxial tilt heating stage, and to ensure accurate measurement of the facet planes the foil was aligned along the common <110> bicrystal zone axis. Figure 5(a-e) is a series of micrographs illustrating the changes observed on a 0.25μm-sized grain subjected to the temperature cycling shown in Figure 5f. After the initial cooling to 200°C the particle was sharply faceted with the segments approximately corresponding to asymmetrical (horizontal and vertical) and symmetrical (diagonal) boundaries. At asymmetrical boundaries (001) planes of one crystal and (110) planes of the other are parallel to the boundary whereas at the symmetrical boundaries $(557)_1/(55\bar{7})_2$ planes are opposite each other.

An unexpected feature is the sharp facet junction of two asymmetric boundaries at the bottom right of the particle meeting at an angle of about 90°. On heating to, and stabilizing at, a temperature of 430°C the overall particle shape became more rounded and the right-angled asymmetric segments were replaced with a symmetric segment (Figure 5b). During subsequent temperature cycles essentially the same reversible sequence was observed, Figure 5(c-e). The ratio of the asymmetric to symmetric boundary length changed from ~2 at 200°C to ~0.8 at 430°C. Closer inspection shows that the asymmetric boundary segments are planar and deviate from the precise $(001)_1/(110)_2$ plane by up to 10° whereas the symmetric regions are more usually broken down into segments deviating by as much as 20° from the exact symmetric $(557)_1/(55\bar{7})_2$ positions. The additional segments were found to correspond to planes with the next highest density of coincidence sites in the Σ99 CSL after the symmetric boundaries.

The initial results of this type of experiment given here show the potential for obtaining useful information on grain boundary "transformations", i.e. faceting and roughening. However, to validate the experiments it will be necessary to collect data from a large number of observations. With such statistical measurements it should be possible to extract data on the relative energies of 90° <110> tilt boundaries as a function of temperature and interface orientation.

The Observation of Facets at the Atomic Level

The ARM at the NCEM currently operates at 800 kV with a point-to-point resolution of better than 1.6Å (12). It is thus possible to clearly resolve the atomic structure of <110> Al bicrystals and observe the core structure of grain boundaries including atomic relaxations. As an example, Figure 6 shows a long facet of a symmetrical boundary that illustrates these points. The atomic structure of each <110> grain of the bicrystal is clearly visible right up to the boundary plane, and the relaxation into structural units with relatively short repeat distance is evident. The boundary lies on the mirror plane between the two crystals, i.e a mirror reflection across the interface plane will change the orientation of each crystal into that of the other. This mirror symmetry and the orientation relationship are directly visible in this high resolution image. A full analysis has confirmed that the boundary is a symmetrical $\Sigma 99$ <110> tilt boundary with a small but measurable rigid body shift characteristic of the relaxed boundary structure. Furthermore, it has recently been possible to calculate structures by both pair potentials and the Embedded Atom Method that closely match the observed experimental image (13).

An atomic resolution image of an asymmetric facet is shown in Figure 7. Again the atomic structure up and into the boundary is remarkably rigid and atomic relaxations are confined to the immediate vicinity of the interface plane. The asymmetry is recognized by the parallel $(001)_1/(110)_2$ planes on each side of the boundary and there is no periodic repeat distance in the boundary, in accordance with the irrational ($\sqrt{2}$) relation between the plane spacings perpendicular to this interface. For the same reason it is difficult to treat this boundary theoretically by computational methods.

Microfaceting

Observation of boundaries at the atomic level occasionally reveal regions where the boundary plane has faceted on a very fine scale. Such regions would appear curved, or flat along a high-index plane when imaged on a coarser scale. An example is given in Figure 8 which shows a high resolution micrograph of a boundary with an average orientation along a $(116)_1$ plane. In this region the boundary is arranged in a sawtooth fashion with $(001)_1$ segments 3 to 4 nm in length in the asymmetrical orientation. The boundary segments connecting the asymmetric facets are nearly parallel to the close parallel (111) plane in the upper crystal. The atomic relaxations in the short planar segments bear the same characteristics as those shown in Fig. 7. Whether this type of microfaceting is an equilibrium effect or is determined by the kinetics or mechanism of boundary motion remains to be established.

Comparison of the Al/Si and Al/Ge Heterophase Interfaces

Cross-sectional TEM specimens of the Al/Si bicrystal structure were prepared to study the nature of the heterophase Al/Si interface both in the as-deposited condition and during in-situ annealing treatments. Figure 9 shows an example of the Si substrate/Al overlayer interface imaged along the common <110> direction in the interface (cf. Figure 2). The interface itself is seen as a horizontal line in the image separating the more open Si from the closely spaced Al structure. The Si lattice below and the Al lattice above the interface are rotated 90° relative to each other such that the boundary orientation can be described as $(001)_{Si}/(110)_{Al}$. Note that this is the same orientation relationship and boundary plane as that of the asymmetrical grain boundary described above with one of the Al grains replaced by a Si grain in identical orientation.

The relaxations in this interface are clearly different than those seen in Figs 7 and 8. There appears to be a periodicity of about 3.6 nm with regions of good registry separated by regions of high distortion. The central region with good registry shows an apparent protrusion of the Al into the Si substrate. Thus the interface may not be atomically flat. However, this image must be interpreted with caution because the different thinning rates of Al and Si during ion milling of the cross section sample can lead to artifacts.

It is of interest to compare the semiconductor/metal interface structure of an ICB sample with a similar interface prepared by other methods. A convenient alternative is provided by the precipitation hardening alloy systems Al-Si and Al-Ge. Following a suitable quench/age treatment the equilibrium structure consists of pure Si or Ge needles precipitated an Al matrix. In each case the needle axis is parallel to a low index zone axis in both the precipitate and matrix, thus satisfying the conditions of Figure 1. A high resolution micrograph of a Ge needle in Al imaged end-on is shown in Figure 10. It is seen that the precipitate has a faceted shape and is internally twinned. Furthermore, the <110> axis of the Ge is accurately parallel to a <100> direction of the Al thus ensuring a clear image of the interface structure. In contrast to the case of the ICB structures it has been observed that the Al/Ge interfaces are rigid, i.e. unrelaxed.

ACKNOWLEDGEMENT

We thank N. Thangaraj, M.A. O'Keefe and J. Turner for the microscopy and image processing on figure 3, J. Douin for figure 10 and C.J.D. Hetherington for figure 7. This work was supported by the Director, Office of Energy Research, Office of Basic Energy Sciences of the U.S. Department of Energy under contract #DE-AC03-76SF00098.

FIGURE CAPTIONS

Figure 1 Schematic diagram illustrating the optimum conditions for imaging a planar interface at high resolution.

Figure 2 Schematic diagram of cross-sectional TEM specimen indicating regions where various observations were made.

Figure 3 Ionized Cluster Beam deposited silver particles showing internal interface formed during either the deposition or subsequent coalescence. (Micrographs taken by N. Thangaraj).

Figure 4 Sketch showing the orientation relationship between the <110> bicrystal Al ICB film and the {100} silicon substrate.

Figure 5 Series of micrographs illustrating changes in shape of an ICB Al grain during temperature cycling.

Figure 6 Atomic resolution image of a symmetric {557} Σ99 <110> tilt boundary in ICB Al.

Figure 7 Atomic resolution image of an asymmetric {100} {011} Σ99 <110> tilt boundary in ICB Al. (Micrograph taken by C.J.D. Hetherington, from ref. 1).

Figure 8 High resolution image of a microfaceted grain boundary in ICB Al.

Figure 9: Atomic resolution image of the interphase boundary between ICB Al and {001} Si substrate.

Figure 10: Micrograph of an end-on Ge precipitate needle in an Al matrix showing the atomic structure at the heterophase interface. (Micrograph by J. Douin).

REFERENCES

1. U. Dahmen, J. Douin, C.J. Hetherington and K.H. Westmacott, MRS Symp. Proc. 139, 87 (1989)

2. M. Turwitt, G. Elssner and G. Petzow, J. de Physique, 46, C4 123, 1985

3. U. Dahmen and K.H. Westmacott, Scripta Metall., 22, 1673 (1988)

4. I.Yamada, H. Inokawa, and T. Takagi, J. Appl. Phys., 56, 2746 (1984).

5. M. Asano, S. Tanaka, H. Usui, I. Yamada and T. Takagi, Proc. 11th Symp. on ISIAT '87, Tokyo (1987), 337

6. M.C. Madden and B.M. Tracy, Proc. 45th Ann. Meeting of EMSA, G. W. Bailey, ed., San Francisco Press, 362 (1987)

7. K.H. Westmacott and U. Dahmen, Proc. ISIAT Conference, Tokyo, Japan (1989)

8. M.L. Sattler and M.A. O'Keefe, Proc. 45th EMSA 104 (1987)

9. M. Flüeli, P.A. Buffat and J.P. Borel, Surf. Sci. 202, 343 (1988)

10. R. Maurer and H. Gleiter, "Experimental Techniques of Texture Analysis", ed. H.J. Bunge, DGM Informationsgesellschaft-Verlag, (1986), p.347

11. Y. Gao, S.A. Dregia and P.G. Shewmon, Acta Met. 37, 1627 (1989)

12. CJ.D. Hetherington, E.C. Nelson, K.H. Westmacott, R. Gronsky and G. Thomas, Proc. MRS Symp. 139, 277 (1989)

13. U. Dahmen, C.J.D. Hetherington, M.A. O'Keefe, K.H. Westmacott, M.J. Mills, M.S. Daw and V. Vitek, submitted to Phys. Rev. Lett.

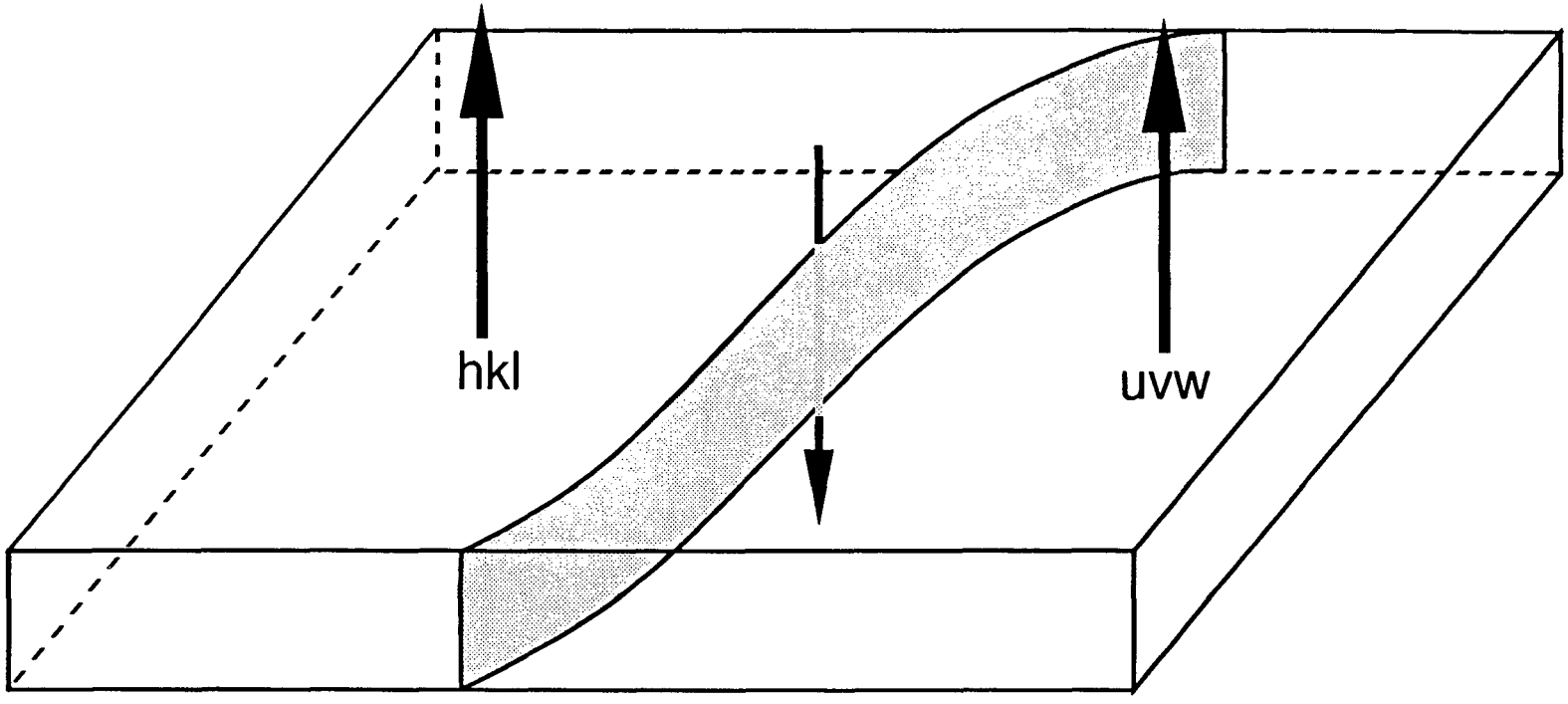

XBL 901-145

FIGURE 1

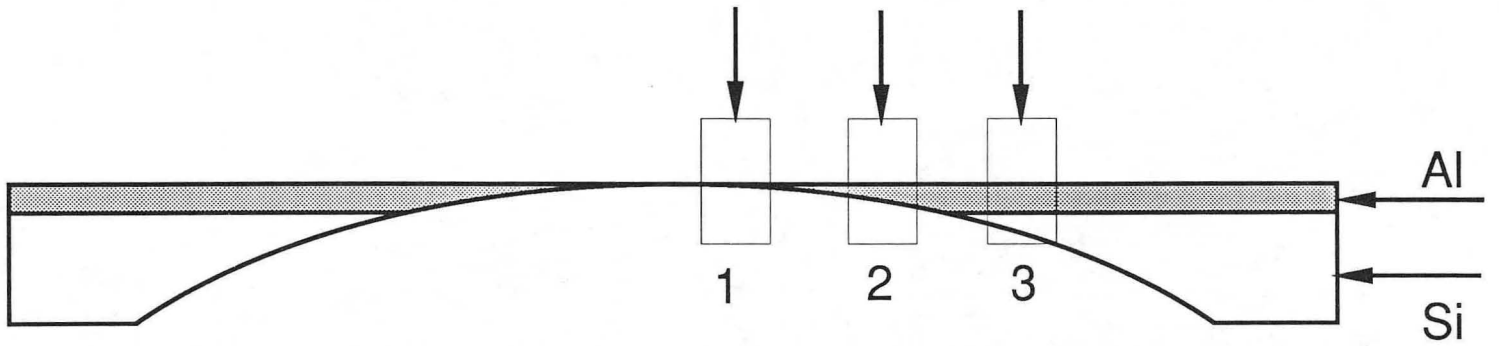

XBL 901-149

FIGURE 2

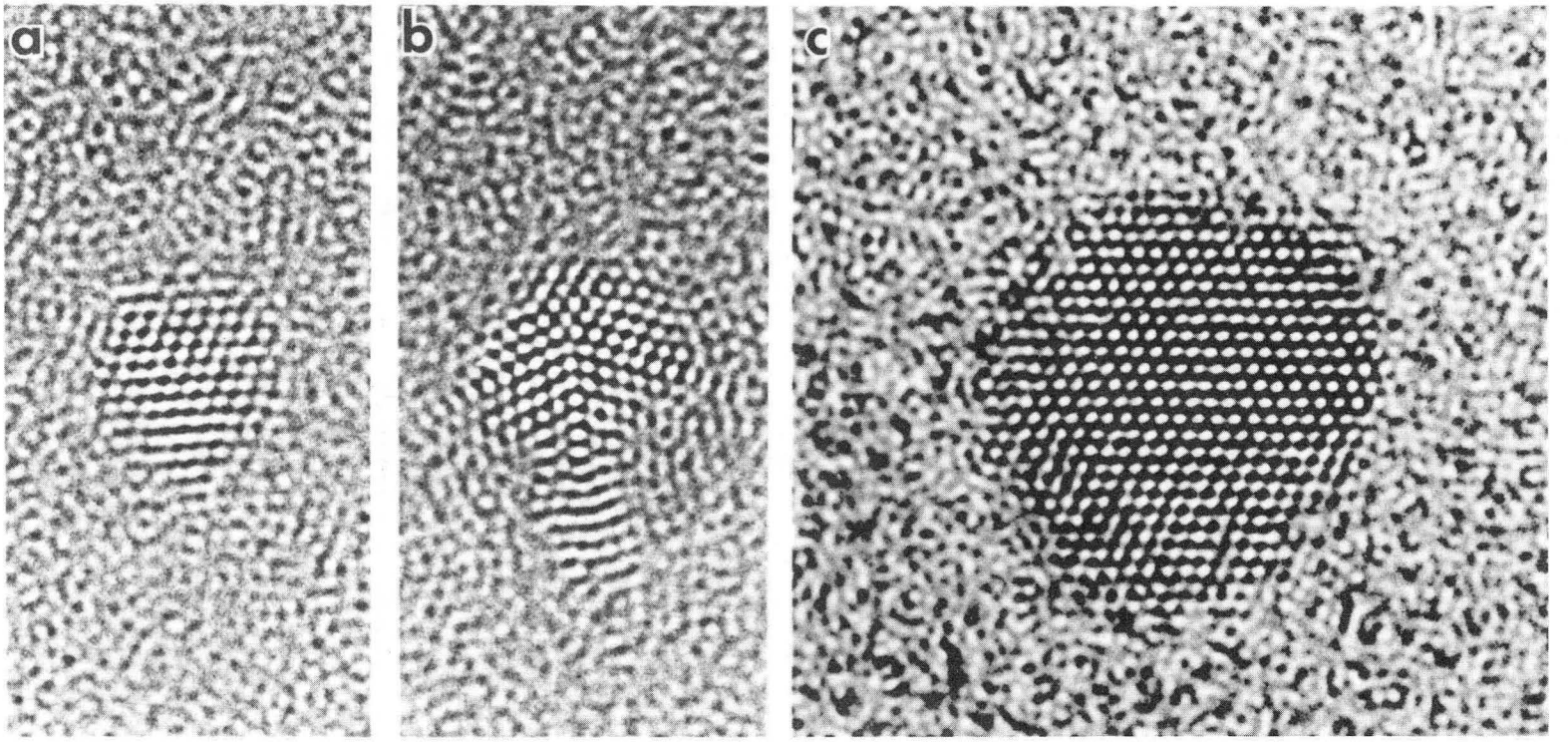

XBB 901-612

FIGURE 3

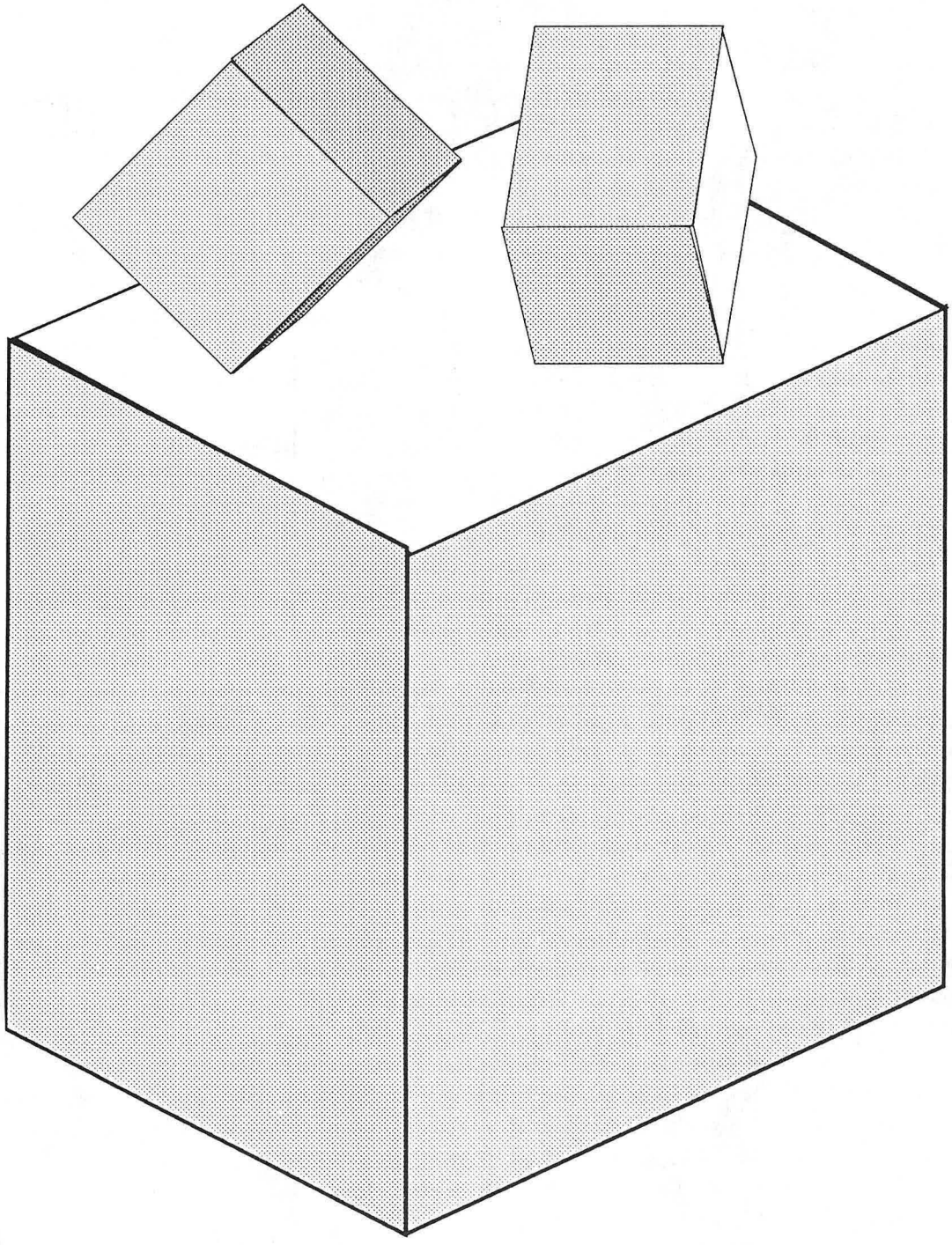

XBL 901-150

FIGURE 4

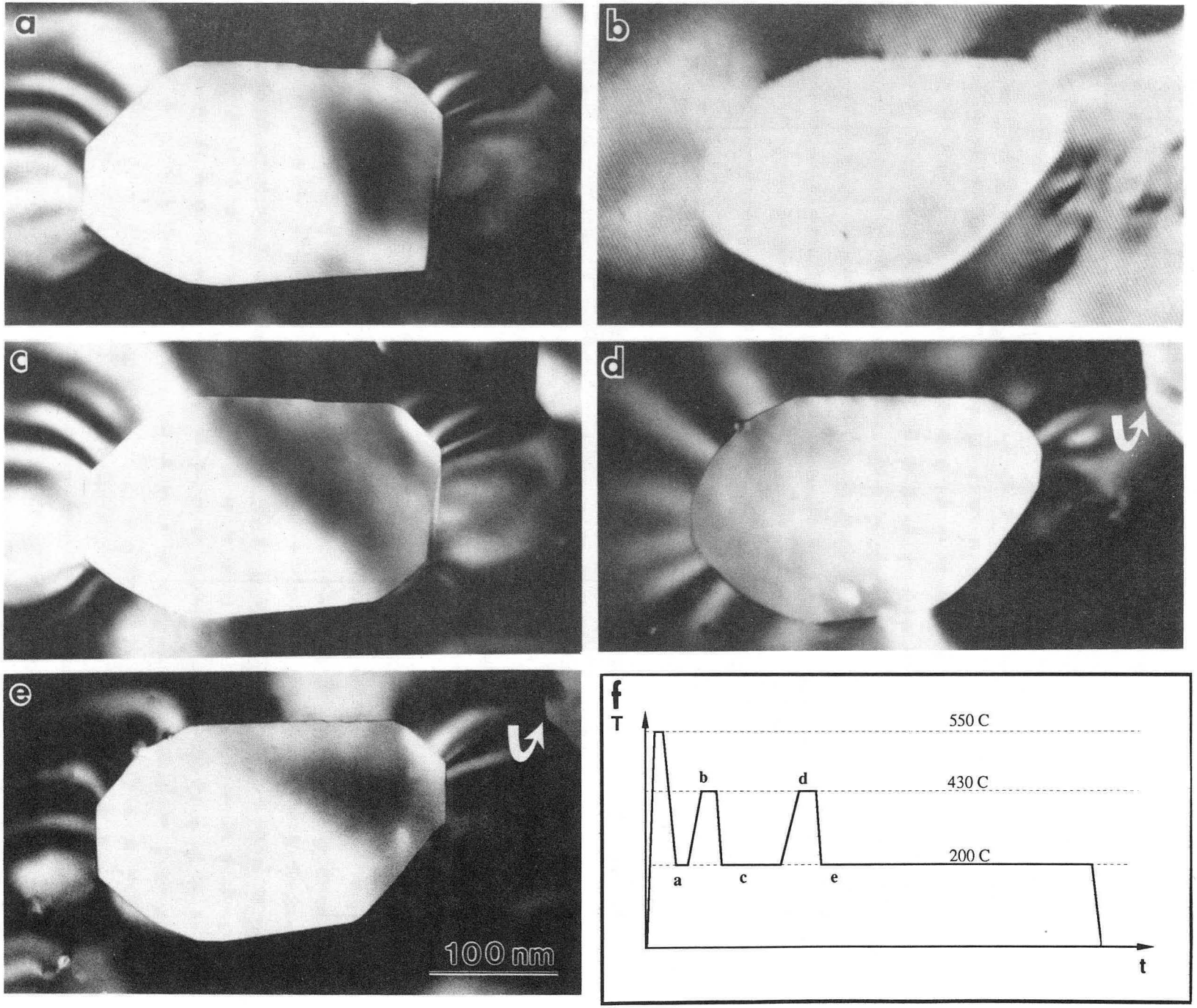

XBB 896-5070

FIGURE 5

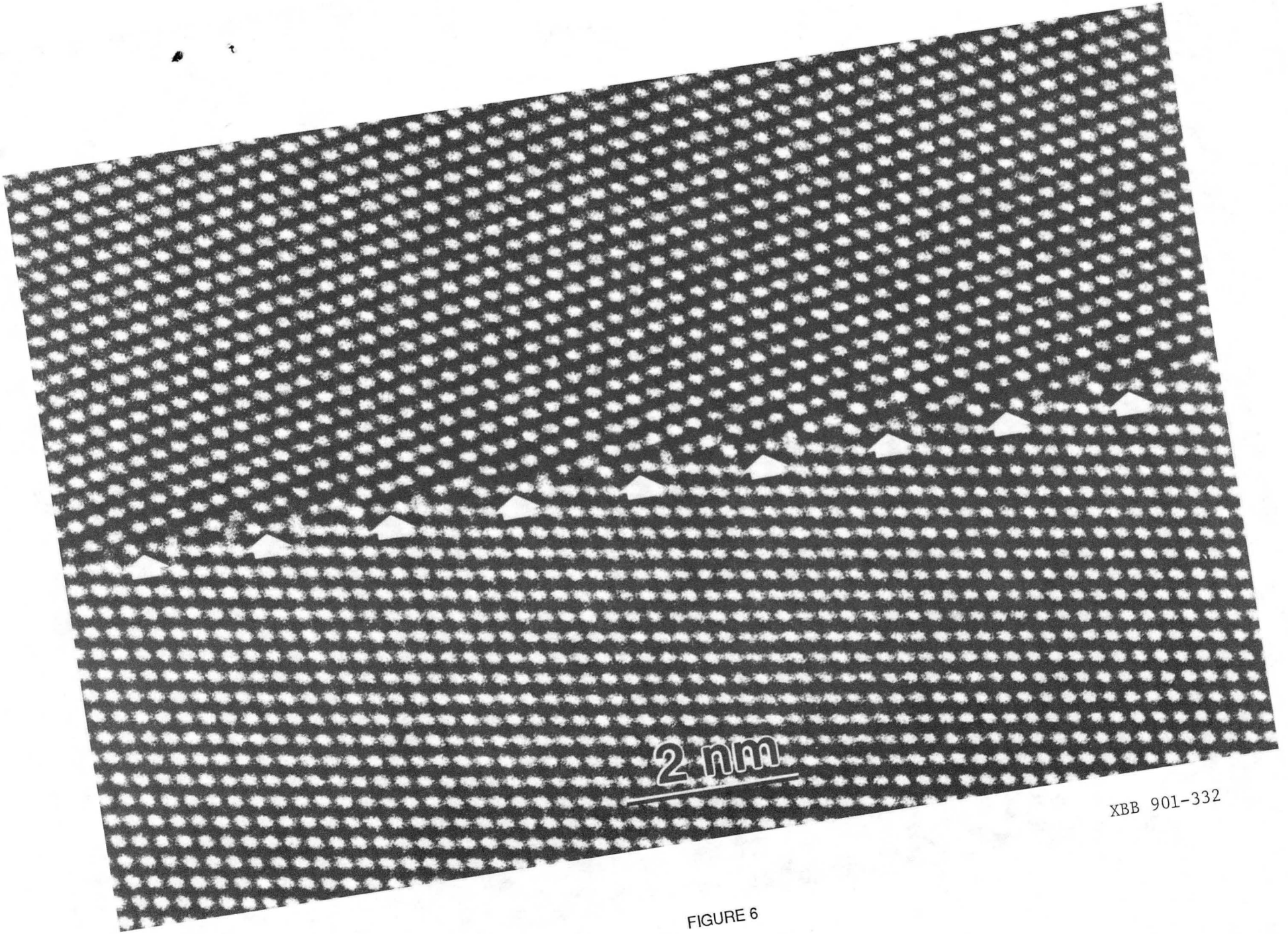

XBB 901-332

FIGURE 6

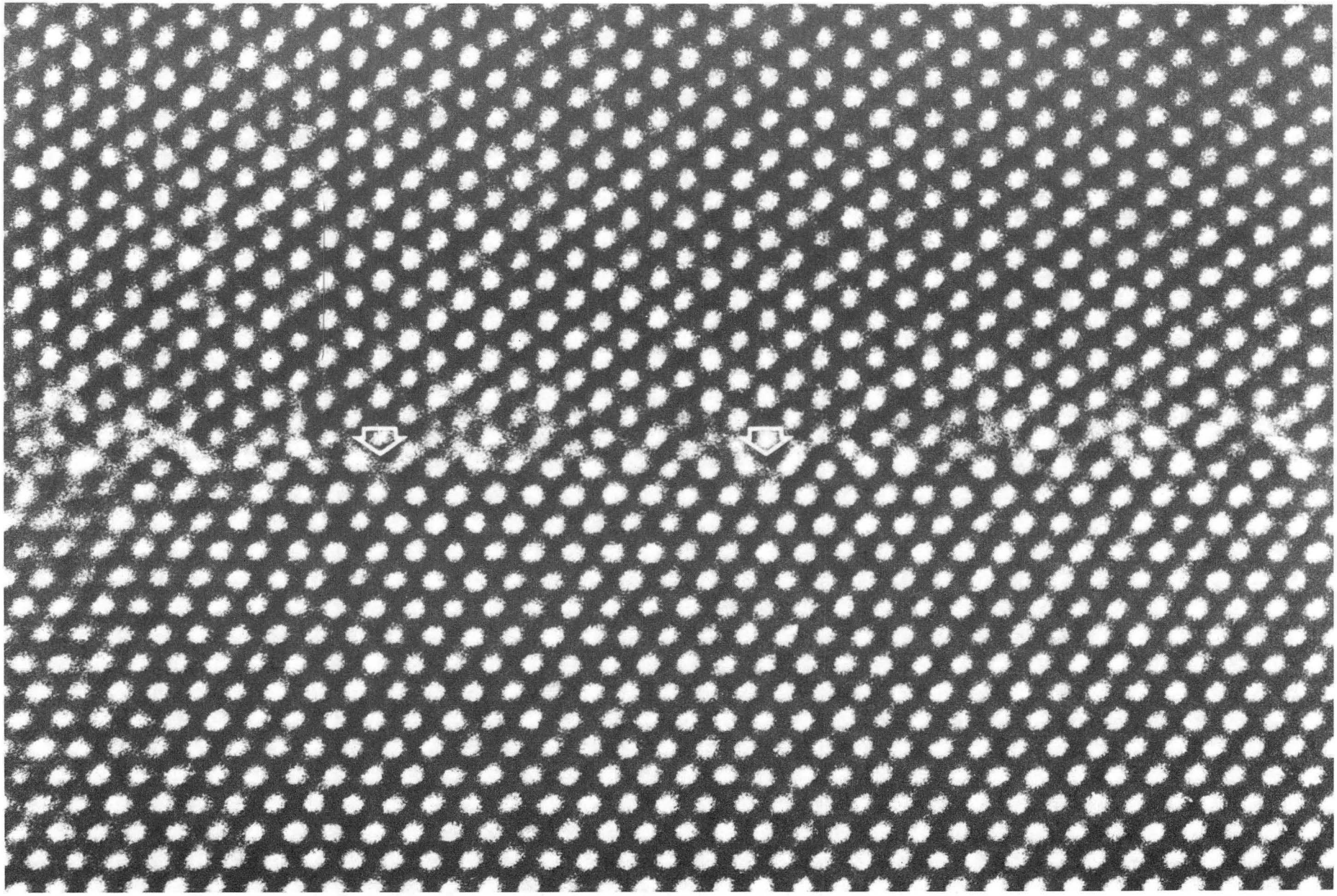

XBB 880-10319

FIGURE 7

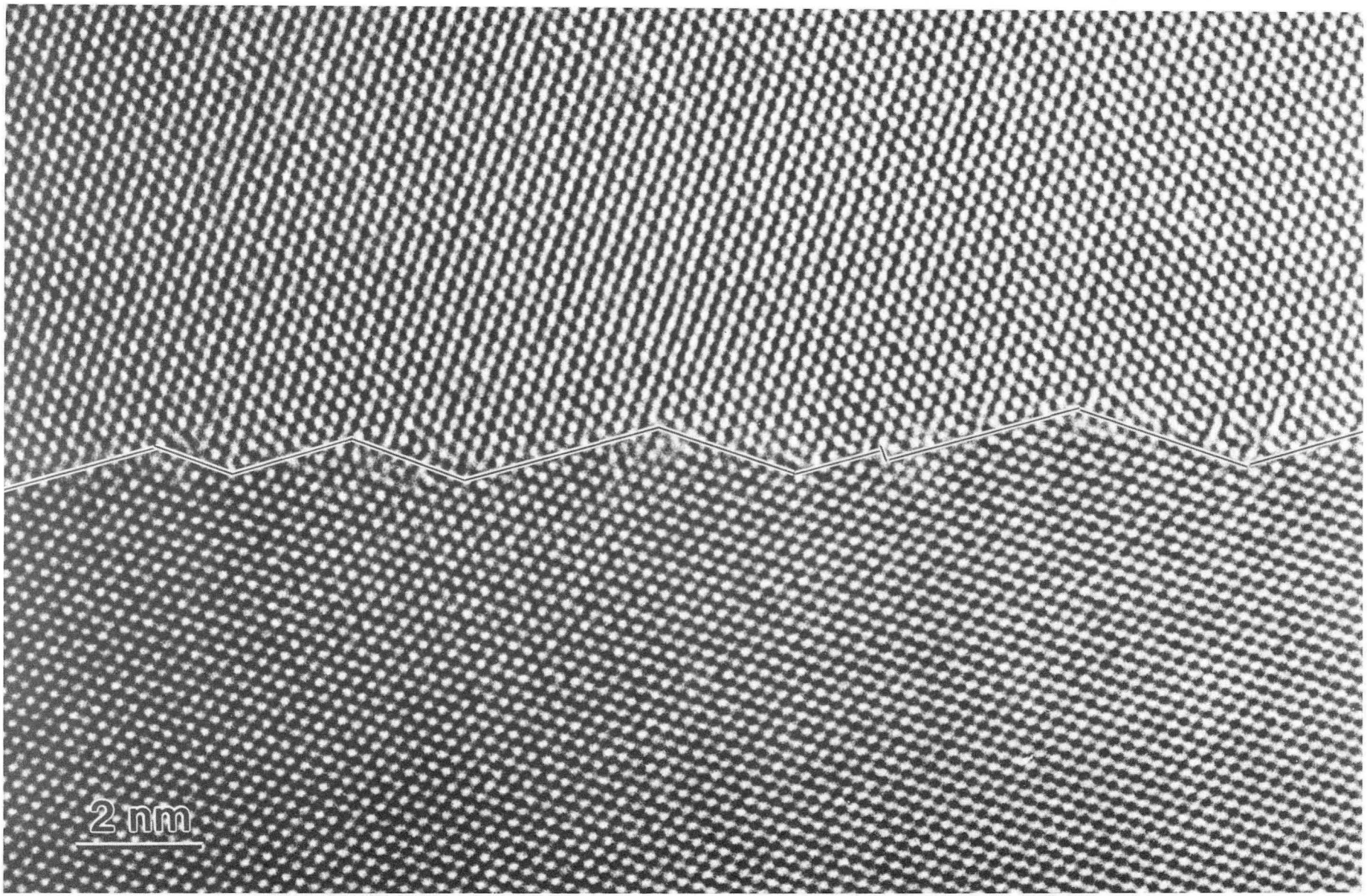

XBB 901-333

FIGURE 8

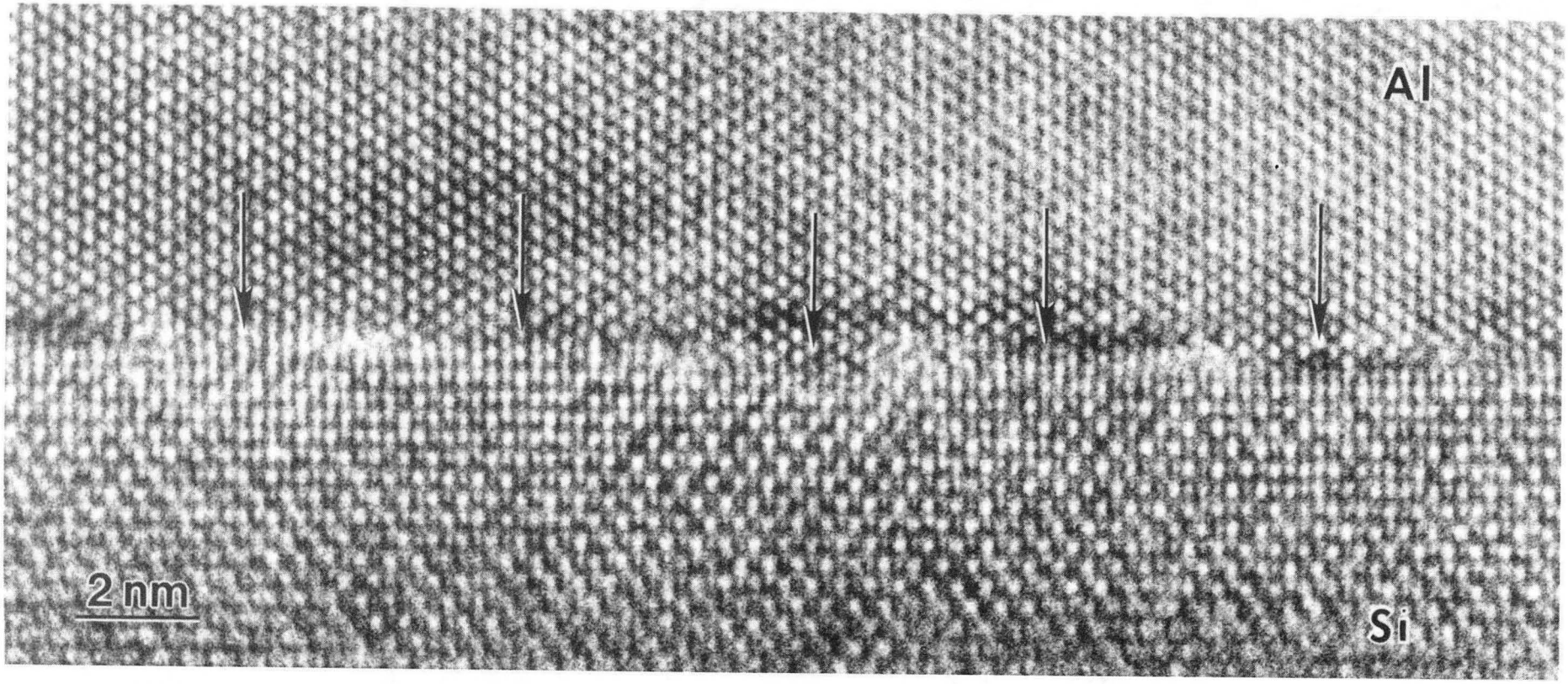

XBB 901-334

FIGURE 9

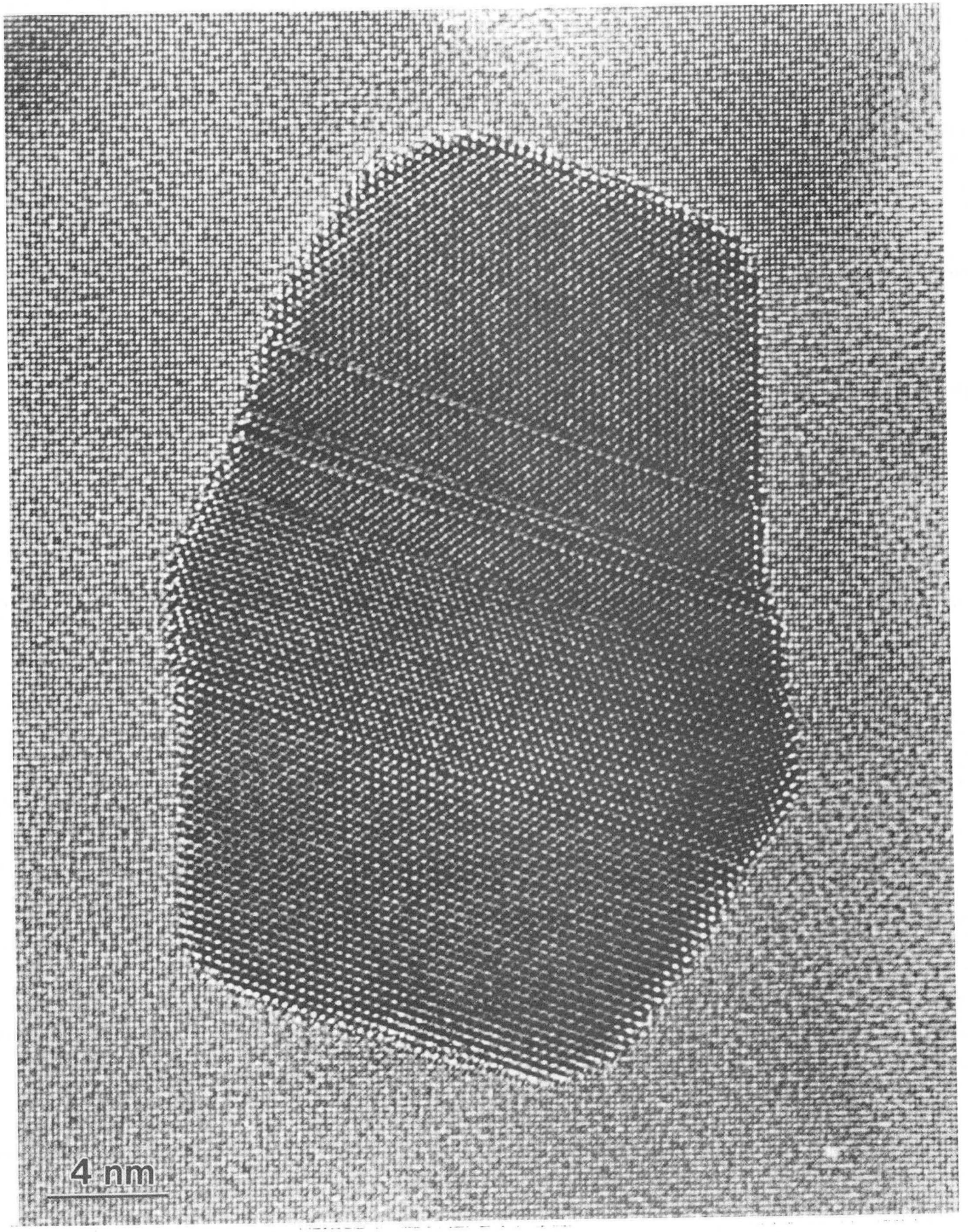

XBB 901-335

FIGURE 10

LAWRENCE BERKELEY LABORATORY
TECHNICAL INFORMATION DEPARTMENT
1 CYCLOTRON ROAD
BERKELEY, CALIFORNIA 94720